

## Striking Antibody Evasion Manifested by the Omicron Variant of SARS-CoV-2

1 Lihong Liu<sup>1\*</sup>, Sho Iketani<sup>1,2\*</sup>, Yicheng Guo<sup>1\*</sup>, Jasper F-W. Chan<sup>3,4\*</sup>, Maple Wang<sup>1\*</sup>, Liyuan  
2 Liu<sup>5\*</sup>, Yang Luo<sup>1</sup>, Hin Chu<sup>3,4</sup>, Yiming Huang<sup>5</sup>, Manoj S. Nair<sup>1</sup>, Jian Yu<sup>1</sup>, Kenn K-H. Chik<sup>4</sup>,  
3 Terrence T-T. Yuen<sup>3</sup>, Chaemin Yoon<sup>3</sup>, Kelvin K-W. To<sup>3,4</sup>, Honglin Chen<sup>3,4</sup>, Michael T. Yin<sup>1,6</sup>,  
4 Magdalena E. Sobieszczyk<sup>1,6</sup>, Yaoxing Huang<sup>1</sup>, Harris H. Wang<sup>5</sup>, Zizhang Sheng<sup>1</sup>,  
5 Kwok-Yung Yuen<sup>3,4</sup>, David D. Ho<sup>1,2,6^</sup>  
6

7 <sup>1</sup>Aaron Diamond AIDS Research Center, Columbia University Vagelos College of Physicians  
8 and Surgeons, New York, NY 10032, USA

9 <sup>2</sup>Department of Microbiology and Immunology, Columbia University Vagelos College of  
10 Physicians and Surgeons, New York, NY 10032, USA

11 <sup>3</sup>State Key Laboratory of Emerging Infectious Diseases, Carol Yu Centre for Infection,  
12 Department of Microbiology, Li Ka Shing Faculty of Medicine, The University of Hong Kong,  
13 Pokfulam, Hong Kong Special Administrative Region, China

14 <sup>4</sup>Centre for Virology, Vaccinology and Therapeutics, Hong Kong Science and Technology Park,  
15 Hong Kong Special Administrative Region, China

16 <sup>5</sup>Department of Systems Biology, Columbia University Vagelos College of Physicians and  
17 Surgeons, New York, NY 10032, USA

18 <sup>6</sup>Division of Infectious Diseases, Department of Medicine, Columbia University Vagelos College  
19 of Physicians and Surgeons, New York, NY 10032, USA  
20

21 \* These authors contributed equally

22 ^ Address correspondence to David D. Ho ([dh2994@cumc.columbia.edu](mailto:dh2994@cumc.columbia.edu), 212-304-6101, 701 W  
23 168th St, 11th Floor, New York, NY 10032)  
24

25 Word count: 3309

26 **Abstract**

27

28 The Omicron (B.1.1.529) variant of SARS-CoV-2 was only recently detected in southern Africa,  
29 but its subsequent spread has been extensive, both regionally and globally<sup>1</sup>. It is expected to  
30 become dominant in the coming weeks<sup>2</sup>, probably due to enhanced transmissibility. A striking  
31 feature of this variant is the large number of spike mutations<sup>3</sup> that pose a threat to the efficacy of  
32 current COVID-19 vaccines and antibody therapies<sup>4</sup>. This concern is amplified by the findings  
33 from our study. We found B.1.1.529 to be markedly resistant to neutralization by serum not only  
34 from convalescent patients, but also from individuals vaccinated with one of the four widely  
35 used COVID-19 vaccines. Even serum from persons vaccinated and boosted with mRNA-based  
36 vaccines exhibited substantially diminished neutralizing activity against B.1.1.529. By  
37 evaluating a panel of monoclonal antibodies to all known epitope clusters on the spike protein,  
38 we noted that the activity of 18 of the 19 antibodies tested were either abolished or impaired,  
39 including ones currently authorized or approved for use in patients. In addition, we also  
40 identified four new spike mutations (S371L, N440K, G446S, and Q493R) that confer greater  
41 antibody resistance to B.1.1.529. The Omicron variant presents a serious threat to many existing  
42 COVID-19 vaccines and therapies, compelling the development of new interventions that  
43 anticipate the evolutionary trajectory of SARS-CoV-2.

44

## 45 **Main text**

46 The COVID-19 pandemic rages on, as the causative agent, SARS-CoV-2, continues to evolve.  
47 Many diverse viral variants have emerged (**Fig. 1a**), each characterized by mutations in the spike  
48 protein that raise concerns of both antibody evasion and enhanced transmission. The Beta  
49 (B.1.351) variant was found to be most refractory to antibody neutralization<sup>4</sup> and thus  
50 compromised the efficacy of vaccines<sup>5-7</sup> and therapeutic antibodies. The Alpha (B.1.1.7) variant  
51 became dominant globally in early 2021 due to an edge in transmission<sup>8</sup> only to be replaced by  
52 the Delta (B.1.617.2) variant, which exhibited even greater propensity to spread coupled with a  
53 moderate level of antibody resistance<sup>9</sup>. Then came the Omicron (B.1.1.529) variant, first  
54 detected in southern Africa in November 2021<sup>3,10,11</sup> (**Fig. 1a**). It has since spread rapidly in the  
55 region, as well as to over 60 countries, gaining traction even where the Delta variant is prevalent.  
56 The short doubling time (2-3 days) of Omicron cases suggests it could become dominant soon<sup>2</sup>.  
57 Moreover, its spike protein contains an alarming number of >30 mutations (**Fig. 1b and**  
58 **Extended Data Fig. 1**), including at least 15 in the receptor-binding domain (RBD), the  
59 principal target for neutralizing antibodies. These extensive spike mutations raise the specter  
60 that current vaccines and therapeutic antibodies would be greatly compromised. This concern is  
61 amplified by the findings we now report.

62

## 63 **Serum neutralization of B.1.1.529**

64 We first examined the neutralizing activity of serum collected in the Spring of 2020 from  
65 COVID-19 patients, who were presumably infected with the wild-type SARS-CoV-2 (see  
66 Methods). Samples from 10 individuals were tested for neutralization against both D614G (WT)  
67 and B.1.1.529 pseudoviruses. While robust titers were observed against D614G, a significant  
68 drop (>32-fold) in ID<sub>50</sub> titers was observed against B.1.1.529, with only 2 samples showing titers  
69 above the limit of detection (LOD) (**Fig. 1c and Extended Data Fig. 2a**). We then assessed the  
70 neutralizing activity of sera from individuals who received one of the four widely used COVID-  
71 19 vaccines: BNT162b2 (Pfizer), mRNA-1273 (Moderna), Ad26.COV2.S (Johnson & Johnson),  
72 and ChAdOx1 nCoV-19 (AstraZeneca) (see Methods and **Extended Data Table 1**). In all cases,  
73 a substantial loss in neutralizing potency was observed against B.1.1.529 (**Fig. 1d and Extended**  
74 **Data Fig. 2b-f**). For the two mRNA-based vaccines, BNT162b2 and mRNA-1273, a >21-fold  
75 and >8.6-fold decrease in ID<sub>50</sub> was seen, respectively. We note that, for these two groups, we

76 specifically chose samples with high titers such that the fold-change in titer could be better  
77 quantified, so the difference in the number of samples having titers above the LOD (6/13 for  
78 BNT162b2 versus 11/12 for mRNA-1273) may be favorably biased. Within the Ad26.COVS2.S  
79 and ChAdOx1 nCoV-19 groups, all samples were below the LOD against B.1.1.529, except for  
80 two Ad26.COVS2.S samples from patients with a previous history of SARS-CoV-2 infection (**Fig.**  
81 **1d**). Collectively, these results suggest that individuals who were previously infected or fully  
82 vaccinated remain at risk for B.1.1.529 infection.

83

84 Booster shots are now routinely administered in many countries 6 months after full vaccination.  
85 Therefore, we also examined the serum neutralizing activity of individuals who had received  
86 three homologous mRNA vaccinations (13 with BNT162b2 and 2 with mRNA-1273). Every  
87 sample showed lower activity in neutralizing B.1.1.529, with a mean drop of 6.5-fold compared  
88 to WT (**Fig. 1d**). Although all samples had titers above the LOD, the substantial loss in activity  
89 may still pose a risk for B.1.1.529 infection despite the booster vaccination.

90

91 We then confirmed the above findings by testing a subset of the BNT162b2 and mRNA-1273  
92 vaccinee serum samples using authentic SARS-CoV-2 isolates: wild type and B.1.1.529. Again,  
93 a substantial decrease in neutralization of B.1.1.529 was observed, with mean drops of >6.0-fold  
94 and >4.1-fold for the fully vaccinated group and the boosted group, respectively (**Fig. 1e**).

95

### 96 **Monoclonal antibody neutralization of B.1.1.529**

97 To understand the types of antibodies in serum that lost neutralizing activity against B.1.1.529,  
98 we assessed the neutralization profile of 19 well-characterized monoclonal antibodies (mAbs) to  
99 the spike protein, including 17 directed to RBD and 2 directed to the N-terminal domain (NTD).  
100 We included mAbs that have been authorized or approved for clinical use, either individually or  
101 in combination: REGN10987 (imdevimab)<sup>12</sup>, REGN10933 (casirivimab)<sup>12</sup>, COV2-2196  
102 (tixagevimab)<sup>13</sup>, COV2-2130 (cilgavimab)<sup>13</sup>, LY-CoV555 (bamlanivimab)<sup>14</sup>, CB6  
103 (etesevimab)<sup>15</sup>, Bii-196 (amubarvimab)<sup>16</sup>, Bii-198 (romlusevimab)<sup>16</sup>, and S309 (sotrovimab)<sup>17</sup>.  
104 We also included other mAbs of interest: 910-30<sup>18</sup>, ADG-2<sup>19</sup>, DH1047<sup>20</sup>, S2X259<sup>21</sup>, and our  
105 antibodies 1-20, 2-15, 2-7, 4-18, 5-7, and 10-40<sup>22-24</sup>. The footprints of mAbs with structures  
106 available were drawn in relation to the mutations found in B.1.1.529 RBD (**Fig. 2a**) and NTD

107 **(Fig. 2b)**. The risk to each of the 4 classes<sup>25</sup> of RBD mAbs, as well as to the NTD mAbs, was  
108 immediately apparent. Indeed, neutralization studies on B.1.1.529 pseudovirus showed that 18  
109 of the 19 mAbs tested lost neutralizing activity completely or partially (**Fig. 2c and Extended**  
110 **Data Fig. 3**). The potency of class 1 and class 2 RBD mAbs all dropped by >100-fold, as did the  
111 more potent mAbs in RBD class 3 (REGN10987, COV2-2130, and 2-7). The activity of S309  
112 declined modestly, whereas Brie-198 was spared. All mAbs in RBD class 4 lost neutralization  
113 potency against B.1.1.529 by at least 10-fold, as did mAb directed to the antigenic supersite<sup>26</sup> (4-  
114 18) or the alternate site<sup>23</sup> (5-7) on NTD. Strikingly, all four combination mAb drugs in clinical  
115 use lost substantial activity against B.1.1.529, likely abolishing or impairing their efficacy in  
116 patients.

117  
118 Approximately 10% of the B.1.1.529 viruses in GISAID<sup>1</sup> also contain an additional RBD  
119 mutation, R346K, which is the defining mutation for the Mu (B.1.621) variant<sup>27</sup>. We therefore  
120 constructed another pseudovirus (B.1.1.529+R346K) containing this mutation for additional  
121 testing using the same panel of mAbs (**Fig. 2d**). The overall findings resembled those already  
122 shown in **Fig. 2c**, with the exception that the neutralizing activities of S309 and Brie198 were  
123 further diminished or abolished. In fact, the entire panel of antibodies was essentially rendered  
124 inactive against this minor form of the Omicron variant.

125  
126 The fold changes in IC<sub>50</sub> of the mAbs against B.1.1.529 and B.1.1.529+R346K relative to  
127 D614G are summarized in the first two rows of **Fig. 3a**. The remarkable loss of activity  
128 observed for all classes of mAbs against B.1.1.529 suggest that perhaps the same is occurring in  
129 the serum of convalescent patients and vaccinated individuals.

130

### 131 **Key mutations conferring antibody resistance**

132 To understand the specific B.1.1.529 mutations that confer antibody resistance, we next tested  
133 individually the same panel of 19 mAbs against pseudoviruses for each of the 34 mutations  
134 (excluding D614G) found in B.1.1.529 or B.1.1.529+R346K. Our findings not only confirmed  
135 the role of known mutations at spike residues 142-145, 417, 484, and 501 in conferring  
136 resistance to NTD or RBD (class 1 or class 2) antibodies<sup>4</sup> but also revealed several mutations  
137 that were previously not known to have functional importance (**Fig. 3a and Extended Data Fig.**

138 4). Q493R mediated resistance to CB6 (class 1) as well as to LY-CoV555 and 2-15 (class 2),  
139 findings that could be explained by the abolishment of hydrogen bonds due to the long side chain  
140 of arginine and induced steric clashes with CDRH3 in these antibodies (**Fig. 3b, left panels**).  
141 Both N440K and G446S mediated resistance to REGN10987 and 2-7 (class 3), observations that  
142 could also be explained by steric hindrance (**Fig. 3b, middle panels**). The most striking and  
143 perhaps unexpected finding was that S371L broadly affected neutralization by mAbs in all 4  
144 RBD classes (**Fig. 3a and Extended Data Fig. 4**). While the precise mechanism of this  
145 resistance is unknown, in silico modeling suggested two possibilities (**Fig. 3b, right panels**).  
146 First, in the RBD-down state, mutating Ser to Leu results in an interference with the N343 glycan,  
147 thereby possibly altering its conformation and affecting class 3 antibodies that typically bind this  
148 region. Second, in the RBD-up state, S371L may alter the local conformation of the loop  
149 consisting of S371-S373-S375, thereby affecting the binding of class 4 antibodies that generally  
150 target a portion of this loop (REF 10-40). It is not clear how class 1 and class 2 RBD mAbs are  
151 affected by this mutation.

152

### 153 **Evolution of antibody resistance of SARS-CoV-2 variants**

154 To gain insight into the antibody resistance of B.1.1.529 relative to previous SARS-CoV-2  
155 variants, we evaluated the neutralizing activity of the same panel of neutralizing mAbs against  
156 pseudoviruses for B.1.1.7<sup>8</sup>, B.1.526<sup>28</sup>, B.1.429<sup>29</sup>, B.1.617.2<sup>9</sup>, P.1<sup>30</sup>, and B.1.351<sup>31</sup>. It is evident  
157 from these results (**Fig. 4 and Extended Data Fig. 5**) that previous variants developed resistance  
158 only to NTD antibodies and class 1 and class 2 RBD antibodies. Here B.1.1.529, with or without  
159 R346K, has made a big mutational leap by becoming not only nearly completely resistant to  
160 class 1 and class 2 RBD antibodies, but also substantial resistance to both class 3 and class 4  
161 RBD antibodies. B.1.1.529 is now the most complete “escapee” from neutralization by currently  
162 available antibodies.

163

### 164 **Discussion**

165 The Omicron variant struck fear almost as soon as it was detected to be spreading in South  
166 Africa. That this new variant would transmit more readily has come true in the ensuing weeks<sup>2</sup>.  
167 The extensive mutations found in its spike protein raised concerns that the efficacy of current  
168 COVID-19 vaccines and antibody therapies might be compromised. Indeed, in this study, sera

169 from convalescent patients (**Fig. 1c**) and vaccinees (**Figs. 1d and 1e**) showed markedly reduced  
170 neutralizing activity against B.1.1.529. These findings are in line with emerging clinical data on  
171 the Omicron variant demonstrating higher rates of reinfection<sup>11</sup> and vaccine breakthroughs. In  
172 fact, recent reports showed that the efficacy of two doses of BNT162b2 vaccine has dropped  
173 from over 90% against the original SARS-CoV-2 strain to approximately 40% and 33% against  
174 B.1.1.529 in the United Kingdom<sup>32</sup> and South Africa<sup>33</sup>, respectively. Even a third booster shot  
175 may not adequately protect against Omicron infection<sup>32,34</sup>, but of course it is advisable to do so.  
176 Vaccines that elicited lower neutralizing titers<sup>35,36</sup> are expected to fare worse against B.1.1.529.

177

178 The nature of the loss in serum neutralizing activity against B.1.1.529 could be discerned from  
179 our findings on a panel of mAbs directed to the viral spike. The neutralizing activities of all four  
180 major classes of RBD mAbs and two distinct classes of NTD mAbs are either abolished or  
181 impaired (**Figs. 2c and 2d**). In addition to previously identified mutations that confer antibody  
182 resistance<sup>4</sup>, we have uncovered four new spike mutations with functional consequences. Q493R  
183 confers resistance to some class 1 and class 2 RBD mAbs; N440K and G446S confer resistance  
184 to some class 3 RBD mAbs; and S371L confers global resistance to many RBD mAbs via  
185 mechanisms that are not yet apparent. While performing these mAb studies, we also observed  
186 that all the currently authorized or approved mAb drugs are rendered weak or inactive by  
187 B.1.1.529 (**Figs. 2c and 3a**). In fact, the Omicron variant that contains R346K seemingly  
188 flattens the antibody therapy landscape for COVID-19 (**Fig. 2d and 3a**).

189

190 The scientific community has chased after SARS-CoV-2 variants for a year. As more and more  
191 of them appeared, our interventions directed to the spike became increasingly ineffective. The  
192 Omicron variant has now put an exclamation mark on this point. It is not too far-fetched to think  
193 that this SARS-CoV-2 is now only a mutation or two away from being pan-resistant to current  
194 antibodies, either monoclonal or polyclonal. We must devise strategies that anticipate the  
195 evolutionary direction of the virus and develop agents that target better conserved viral elements.

196 **Figure Legends**

197

198 **Fig. 1. Resistance of B.1.1.529 to neutralization by sera.** **a**, Unrooted phylogenetic tree of  
199 B.1.1.529 with other major SARS-CoV-2 variants. **b**, Key spike mutations found in the viruses  
200 isolated in the major lineage of B.1.1.529 are denoted. **c**, Neutralization of D614G and B.1.1.529  
201 pseudoviruses by convalescent patient sera. **d**, Neutralization of D614G and B.1.1.529  
202 pseudoviruses by vaccinee sera. Within the four standard vaccination groups, individuals that  
203 were vaccinated without documented infection are denoted as circles and individuals that were  
204 both vaccinated and infected are denoted as triangles. Within the boosted group, Moderna  
205 vaccinees are denoted as squares and Pfizer vaccinees are denoted as diamonds. **e**, Neutralization  
206 of authentic D614G and B.1.1.529 viruses by vaccinee sera. Moderna vaccinees are denoted as  
207 squares and Pfizer vaccinees are denoted as diamonds. For all panels, values above the symbols  
208 denote geometric mean titer and the numbers in parentheses denote the sample size. *P* values  
209 were determined by using a Wilcoxon matched-pairs signed-rank test (two-tailed).

210

211 **Fig. 2. Resistance of B.1.1.529 to neutralization by monoclonal antibodies.** **a**, Footprints of  
212 RBD-directed antibodies, with mutations within B.1.1.529 highlighted in cyan. Approved or  
213 authorized antibodies are bolded. The receptor binding motif (RBM) residues are highlighted in  
214 yellow. **b**, Footprints of NTD-directed antibodies, with mutations within B.1.1.529 highlighted in  
215 cyan. The NTD supersite residues are highlighted in light pink. **c**, Neutralization of D614G and  
216 B.1.1.529 pseudoviruses by RBD-directed and NTD-directed mAbs. **d**, Neutralization D614G  
217 and B.1.1.529+R346K pseudoviruses by RBD-directed and NTD-directed mAbs.

218

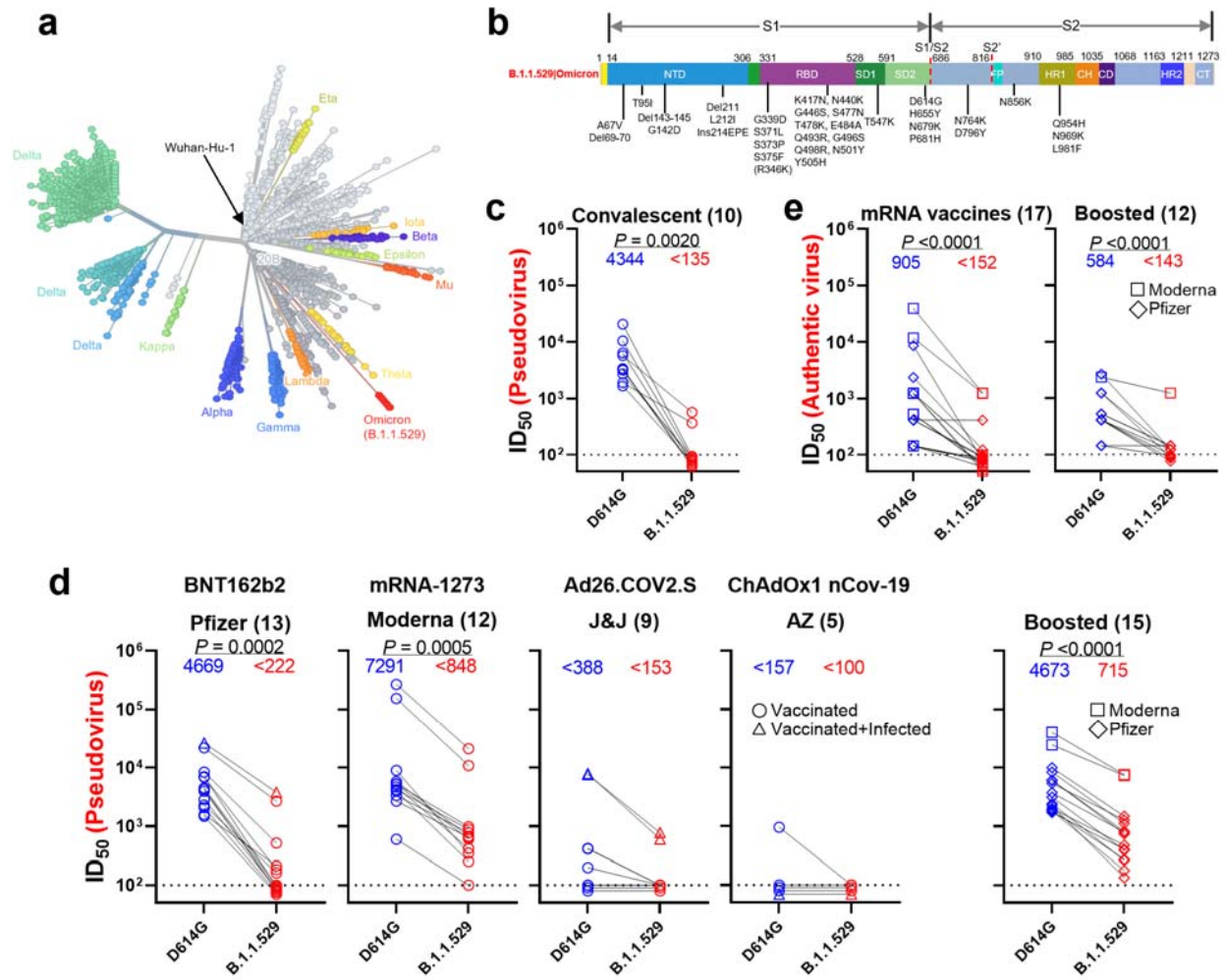
219 **Fig. 3. Impact of individual mutations within B.1.1.529 against monoclonal antibodies.** **a**,  
220 Neutralization of pseudoviruses harboring single mutations found within B.1.1.529 by a panel of  
221 19 monoclonal antibodies. Fold change relative to neutralization of D614G is denoted, with  
222 resistance colored red and sensitization colored green. **b**, Modeling of critical mutations in  
223 B.1.1.529 that affect antibody neutralization.

224



225 **Fig. 4. Evolution of antibody resistance across SARS-CoV-2 variants.** Neutralization of  
226 SARS-CoV-2 variant pseudoviruses by a panel of 19 monoclonal antibodies. Fold change  
227 relative to neutralization of D614G is denoted.  
228

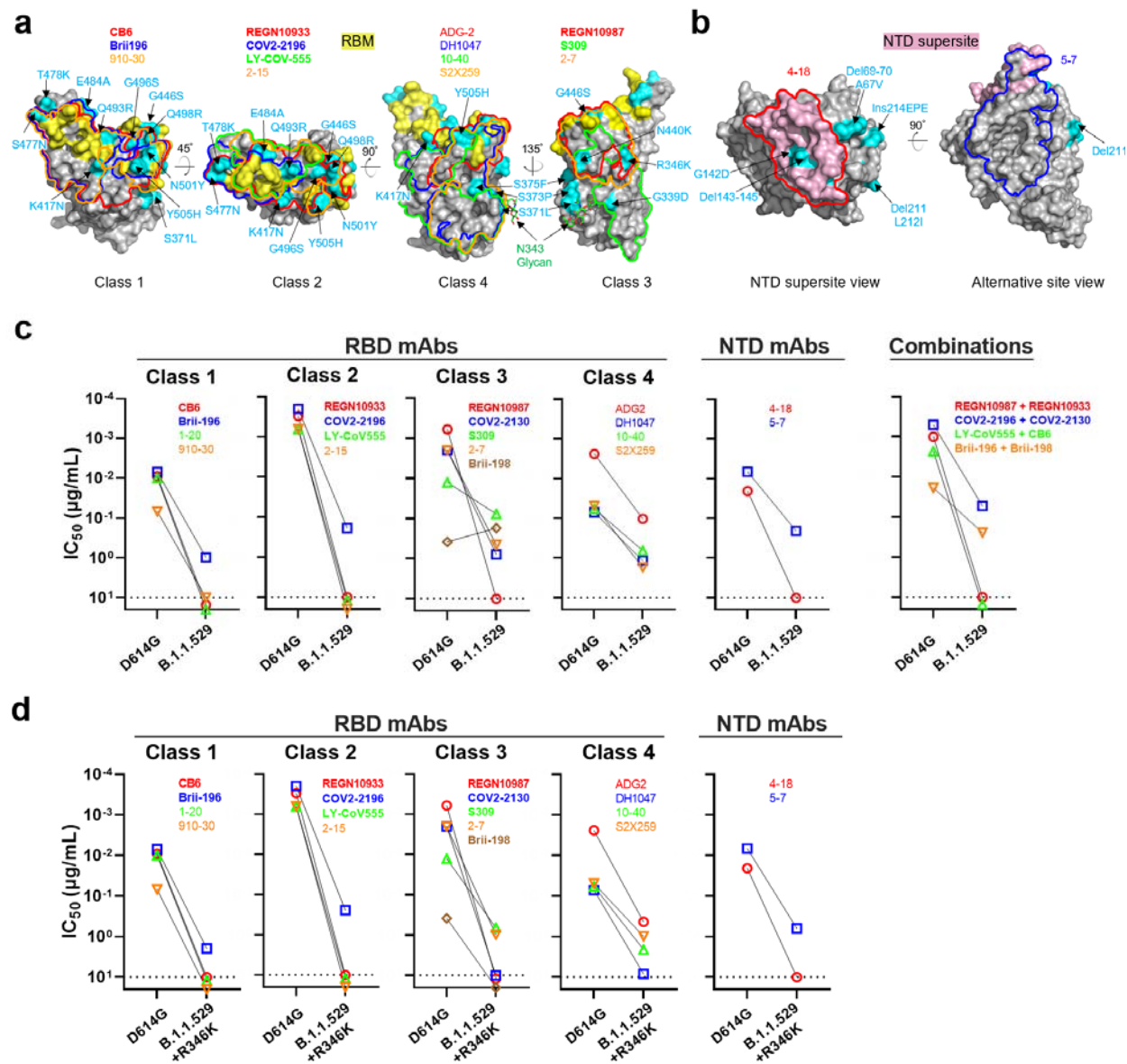
Fig. 1



229

230

**Fig. 2**



231

232

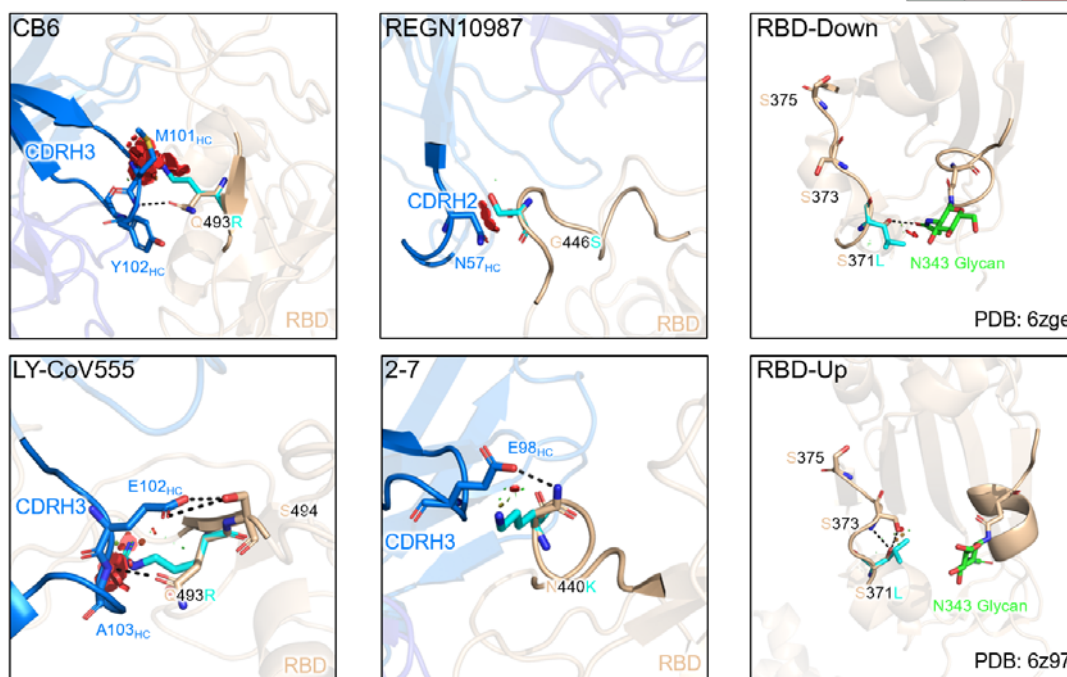
Fig. 3

a

Fold change in IC50 compared with WT	RBD mAbs																NTD mAbs		
	Class 1				Class 2				Class 3				Class 4				4-18	5-7	
	CB6	Brl1-196	1-20	910-30	REGN10933	COV2-2196	LY-CoV555	2-15	REGN10987	COV2-2130	S309	2-7	Brl1-198	ADG-2	DH1047	10-40	S2X259	4-18	5-7
B.1.1.529	<-1000	-134	<-338	<-159	<-1000	-140	<-1000	<-1000	<-1000	-390	-6.1	-231	2.2	-43	-124	-11	-35	-125	-30
B.1.1.529 + R346K	<-761	-97	<-338	<-159	<-1000	-89	<-1000	<-1000	<-1000	<-988	-21	-109	<-32	-51	-167	-32	-16	-125	-33
A67V	1.1	1.0	-1.1	1.4	1.1	-1.0	1.1	1.1	1.1	1.2	-1.4	-1.1	-1.2	1.3	-1.3	-1.1	1.0	-1.6	-1.1
Del169-70	-1.4	-1.4	-1.6	-1.1	-1.8	-1.5	-1.4	-1.4	-1.7	-1.4	-2.2	-1.9	-2.3	-1.4	-3.3	-1.7	-1.3	-2.6	-9.4
T95I	-1.4	-2.0	-1.8	-1.7	-1.5	-1.6	-1.5	1.1	-2.0	-1.1	-2.3	-3.4	1.3	-2.5	-3.4	-1.9	-2.2	1.0	-9.5
G142D	-1.3	-1.4	-1.6	1.0	-1.6	-1.6	-1.7	-1.6	-1.9	-1.5	-2.9	-2.9	-1.5	-1.4	-2.8	-1.4	-1.5	<-125	-263
Del143-145	1.3	1.0	-1.2	1.4	1.3	1.6	1.3	1.5	1.1	-1.1	-1.9	1.2	-1.3	1.2	-2.0	-1.2	<-125	-29	
Del211	-2.4	-2.1	-1.6	-2.1	-1.5	-1.5	-1.4	-1.2	1.2	-1.2	-1.2	-1.3	-1.1	-1.9	-2.4	-1.6	-2.3	1.2	-9.1
L212I	-1.3	-1.8	-1.3	-1.6	-1.4	-1.4	-1.6	-1.3	-1.3	-1.4	-2.2	-1.9	-2.2	-1.7	-3.2	-2.0	-1.9	-7.2	-2.2
Ins214EPE	-2.4	-2.4	-2.2	-2.4	-2.8	-2.7	-2.3	-4.3	-3.0	-2.2	-3.0	-6.2	-2.7	-3.1	-2.9	-1.9	-3.3	-7.1	-15
G339D	-1.7	-1.6	-1.7	-1.4	-2.2	-1.7	-1.5	-1.4	-1.8	-1.6	-4.0	-1.9	-3.9	-1.6	-2.2	-1.5	-3.2	-4.5	-3.0
(R346K)	-1.5	-1.2	-1.3	1.0	-1.5	-1.3	-1.3	-1.4	-1.6	-2.9	-1.4	-1.0	-2.1	-1.1	-1.9	-1.2	-1.4	-1.4	-2.3
S371L	-19	-18	-15	-22	-10	-4.1	-2.9	-1.4	-25	-1.4	-12	-17	-18	-49	-59	-2.4	-23	-1.8	1.1
S373P	-1.9	-2.1	-1.6	-1.4	-1.9	-2.1	-2.0	-1.4	-1.9	-1.3	-2.3	-1.8	-2.5	-2.2	-5.1	-5.0	-2.8	-8.2	-5.0
S375F	1.7	1.6	1.6	1.5	2.1	1.9	1.9	2.6	1.2	1.5	-1.1	1.4	1.1	1.8	-1.8	-1.2	-1.6	-9.2	-1.6
K417N	<-761	-1.6	-2.3	<-158	-6.4	1.1	1.5	1.1	1.2	1.2	-1.8	1.5	-1.0	-1.1	-1.9	-1.5	-1.8	-5.3	-2.8
N440K	-1.4	-1.4	-1.6	-1.2	-1.7	-1.4	-1.4	-1.6	-246	-1.5	-2.3	-18	-1.6	1.1	-2.0	-1.3	-1.5	-4.3	-2.8
G446S	1.3	1.1	-1.1	1.2	-1.6	-1.1	-1.6	-3.0	-574	-3.7	-1.7	-50	-1.4	-1.6	-2.2	-1.4	-2.2	-3.9	-2.4
S477N	-1.8	-1.8	-1.7	-1.7	-2.4	-1.5	-1.5	-1.7	-2.9	-1.6	-1.9	-4.4	-2.4	-1.5	-2.3	-1.6	-2.2	-17	-5.1
T478K	1.2	1.1	1.4	1.6	1.3	-1.5	-1.4	-1.2	-1.6	1.1	-1.8	-2.6	-1.6	-1.2	-2.8	-1.3	-2.3	-3.3	-2.3
E484A	-2.8	-1.7	-1.8	-1.2	-4.8	-4.9	<-1000	<-1000	-1.6	-1.4	-1.4	-2.7	-1.9	-1.6	-1.5	-1.9	-1.9	-5.7	-2.9
Q493R	-16	-7.3	-3.2	2.9	-42	-4.2	<-1000	-705	-1.4	-1.1	-1.2	-1.9	-2.0	-1.6	-1.6	-1.6	-1.5	-4.0	-1.3
G496S	-1.3	1.3	1.1	1.1	1.0	1.1	1.0	-9.3	-6.2	-1.3	-1.4	1.4	-1.2	-1.2	-1.6	-1.1	-1.6	-2.6	-1.6
Q498R	-1.7	-1.2	1.1	1.4	-1.5	-1.1	-1.4	-1.0	-1.6	-1.4	-1.3	1.1	-1.2	2.4	-1.3	-1.2	-1.3	-1.5	-1.8
N501Y	-9.8	-1.2	-8.4	-16	-1.4	-1.5	-1.6	-1.2	-1.2	-1.1	-1.8	-1.5	-2.7	-1.8	-2.5	-1.9	-1.9	-20	-3.9
Y505H	-1.2	1.2	-1.3	-9.6	1.1	1.0	1.0	1.1	1.4	1.0	-1.4	1.7	1.1	1.3	-1.4	1.0	-1.2	-1.2	-1.1
T547K	-1.9	-2.0	-2.0	-1.9	-1.7	-1.3	-1.6	-1.7	-2.7	-1.6	-1.6	-4.3	-1.9	-1.7	-2.6	-1.5	-1.9	-2.7	-2.7
H655Y	-2.7	-3.1	-3.5	-2.7	-3.1	-2.0	-2.2	-8.6	-8.8	-1.7	-2.3	-13	-2.4	-2.1	-3.9	-3.3	-3.9	-23	-5.3
N679K	1.0	1.2	1.1	1.1	-1.1	-1.2	-1.2	-1.2	-1.9	-1.1	-1.3	-1.8	-1.7	-1.4	-2.4	-1.7	-1.7	-2.1	-2.7
P681H	-2.3	-2.1	-2.1	1.0	-2.4	-1.8	-2.2	-1.5	-1.5	-1.0	-1.6	-1.9	-1.5	-1.3	-2.3	-1.3	-1.3	-2.3	-2.4
N764K	-1.1	-1.5	-1.3	-1.1	-1.4	-1.4	-1.4	-2.1	-2.5	-1.5	-2.2	-4.3	-1.3	-1.4	-3.3	-2.1	-2.4	-2.3	-2.1
D769Y	1.3	1.1	1.0	1.2	-1.5	-1.0	-1.4	-1.4	-2.0	-1.3	-1.9	-2.5	-1.3	-1.1	-1.7	-1.2	-1.4	-3.1	-2.5
N856K	-10	-2.8	-1.3	-12	-2.2	-3.0	-1.1	-1.0	-1.4	-1.1	-1.2	-1.3	-2.3	-1.8	-4.4	-2.1	-2.5	-1.6	-1.9
Q954H	2.7	1.9	1.5	2.6	1.2	1.0	1.2	1.1	-1.1	1.2	-1.2	-1.4	-1.1	-1.1	-2.5	-1.0	-1.1	-2.3	-2.9
N969K	-5.4	-1.6	-1.1	-4.5	-1.3	-1.8	-1.1	-1.3	-1.6	-1.1	-1.4	-2.4	-1.4	-1.1	-2.3	-2.0	-2.4	-2.5	-2.0
L981F	3.2	3.3	2.1	4.6	2.4	2.5	2.2	1.9	1.3	2.5	-1.0	-1.5	8.6	2.8	1.1	2.0	2.1	-1.3	-1.5

Legend: >3 <-3 <-10 <-100

b



233

234

Fig. 4

Fold change in IC50 compared with WT	RBD mAbs																NTD mAbs		
	Class 1				Class 2				Class 3				Class 4				4-18	5-7	
	CB6	Bril-196	1-20	910-30	REGN10833	COV2-2196	LY-CoV555	2-15	REGN10887	COV2-2130	S309	2-7	Bril-198	ADG-2	DH1047	10-40			S2X259
<b>B.1.1.7</b>	-8.8	2.6	-5.2	-15	1.6	1.8	1.6	2.2	2.9	1.7	1.1	2.3	4.1	1.7	2.2	1.4	1.4	-5.1	-4.0
<b>B.1.526</b>	-1.0	1.1	-1.1	2.5	-4.5	-2.1	-590	-1329	1.8	1.2	2.9	1.8	-1.1	1.5	2.9	-2.2	1.4	4.5	-2.5
<b>B.1.429</b>	3.0	2.3	1.4	2.5	2.5	2.8	-590	-4.6	1.6	1.1	1.9	1.6	-2.4	2.0	2.9	1.3	3.3	-39	-59
<b>B.1.617.2</b>	2.1	1.2	-1.1	2.5	1.2	1.4	-590	-10	-1.8	-1.7	1.2	-1.1	-8.9	1.0	1.4	-1.8	-1.4	-39	-74
<b>P.1</b>	-196	2.2	-16	-60	-121	-2.0	-590	-1329	1.9	1.1	1.1	1.2	1.8	-1.0	3.0	-2.2	1.2	-39	-74
<b>B.1.351</b>	-196	2.0	-40	-60	-78	-2.5	-590	-1329	1.5	1.5	1.2	1.9	-1.5	1.0	3.0	-2.9	1.2	-39	-8.4
<b>B.1.1.529</b>	<-1000	-134	<-338	<-159	<-1000	-140	<-1000	<-1000	<-1000	-390	-6.1	-231	2.2	-43	-124	-11	-35	-125	-30
<b>B.1.1.529 + R346K</b>	<-761	-97	<-338	<-159	<-1000	-89	<-1000	<-1000	<-1000	<-988	-21	-109	<-32	-51	-167	-32	-16	-125	-33

Legend: >3 <-3 <-10 <-100

235

236 **References**

237

- 238 1 Shu, Y. & McCauley, J. GISAID: Global initiative on sharing all influenza data - from  
239 vision to reality. *Euro Surveill* **22**, doi:10.2807/1560-7917.ES.2017.22.13.30494 (2017).
- 240 2 Grabowski, F., Kochańczyk, M. & Lipniacki, T. Omicron strain spreads with the  
241 doubling time of 3.2—3.6 days in South Africa province of Gauteng that achieved herd  
242 immunity to Delta variant. *medRxiv*, doi:<https://doi.org/10.1101/2021.12.08.21267494>  
243 (2021).
- 244 3 Scott, L. *et al.* Track Omicron's spread with molecular data. *Science*, eabn4543,  
245 doi:10.1126/science.abn4543 (2021).
- 246 4 Wang, P. *et al.* Antibody resistance of SARS-CoV-2 variants B.1.351 and B.1.1.7.  
247 *Nature* **593**, 130-135, doi:10.1038/s41586-021-03398-2 (2021).
- 248 5 Abu-Raddad, L. J., Chemaitelly, H., Butt, A. A. & National Study Group for, C.-V.  
249 Effectiveness of the BNT162b2 Covid-19 Vaccine against the B.1.1.7 and B.1.351  
250 Variants. *N Engl J Med* **385**, 187-189, doi:10.1056/NEJMc2104974 (2021).
- 251 6 Madhi, S. A. *et al.* Efficacy of the ChAdOx1 nCoV-19 Covid-19 Vaccine against the  
252 B.1.351 Variant. *N Engl J Med* **384**, 1885-1898, doi:10.1056/NEJMoa2102214 (2021).
- 253 7 Sadoff, J. *et al.* Safety and Efficacy of Single-Dose Ad26.COV2.S Vaccine against  
254 Covid-19. *N Engl J Med* **384**, 2187-2201, doi:10.1056/NEJMoa2101544 (2021).
- 255 8 Davies, N. G. *et al.* Estimated transmissibility and impact of SARS-CoV-2 lineage  
256 B.1.1.7 in England. *Science* **372**, doi:10.1126/science.abg3055 (2021).
- 257 9 Mlcochova, P. *et al.* SARS-CoV-2 B.1.617.2 Delta variant replication and immune  
258 evasion. *Nature* **599**, 114-119, doi:10.1038/s41586-021-03944-y (2021).
- 259 10 Hadfield, J. *et al.* Nextstrain: real-time tracking of pathogen evolution. *Bioinformatics* **34**,  
260 4121-4123, doi:10.1093/bioinformatics/bty407 (2018).
- 261 11 Pulliam, J. R. C. *et al.* Increased risk of SARS-CoV-2 reinfection associated with  
262 emergence of the Omicron variant in South Africa. *medRxiv*,  
263 doi:<https://doi.org/10.1101/2021.11.11.21266068> (2021).
- 264 12 Hansen, J. *et al.* Studies in humanized mice and convalescent humans yield a SARS-  
265 CoV-2 antibody cocktail. *Science* **369**, 1010-1014, doi:10.1126/science.abd0827 (2020).

- 266 13 Zost, S. J. *et al.* Potently neutralizing and protective human antibodies against SARS-  
267 CoV-2. *Nature* **584**, 443-449, doi:10.1038/s41586-020-2548-6 (2020).
- 268 14 Jones, B. E. *et al.* The neutralizing antibody, LY-CoV555, protects against SARS-CoV-2  
269 infection in nonhuman primates. *Sci Transl Med* **13**, doi:10.1126/scitranslmed.abf1906  
270 (2021).
- 271 15 Shi, R. *et al.* A human neutralizing antibody targets the receptor-binding site of SARS-  
272 CoV-2. *Nature* **584**, 120-124, doi:10.1038/s41586-020-2381-y (2020).
- 273 16 Ju, B. *et al.* Human neutralizing antibodies elicited by SARS-CoV-2 infection. *Nature*  
274 **584**, 115-119, doi:10.1038/s41586-020-2380-z (2020).
- 275 17 Pinto, D. *et al.* Cross-neutralization of SARS-CoV-2 by a human monoclonal SARS-CoV  
276 antibody. *Nature* **583**, 290-295, doi:10.1038/s41586-020-2349-y (2020).
- 277 18 Banach, B. B. *et al.* Paired heavy- and light-chain signatures contribute to potent SARS-  
278 CoV-2 neutralization in public antibody responses. *Cell Rep* **37**, 109771,  
279 doi:10.1016/j.celrep.2021.109771 (2021).
- 280 19 Rappazzo, C. G. *et al.* Broad and potent activity against SARS-like viruses by an  
281 engineered human monoclonal antibody. *Science* **371**, 823-829,  
282 doi:10.1126/science.abf4830 (2021).
- 283 20 Li, D. *et al.* In vitro and in vivo functions of SARS-CoV-2 infection-enhancing and  
284 neutralizing antibodies. *Cell* **184**, 4203-4219 e4232, doi:10.1016/j.cell.2021.06.021  
285 (2021).
- 286 21 Tortorici, M. A. *et al.* Broad sarbecovirus neutralization by a human monoclonal  
287 antibody. *Nature* **597**, 103-108, doi:10.1038/s41586-021-03817-4 (2021).
- 288 22 Liu, L. *et al.* Potent neutralizing antibodies against multiple epitopes on SARS-CoV-2  
289 spike. *Nature* **584**, 450-456, doi:10.1038/s41586-020-2571-7 (2020).
- 290 23 Cerutti, G. *et al.* Neutralizing antibody 5-7 defines a distinct site of vulnerability in  
291 SARS-CoV-2 spike N-terminal domain. *Cell Rep* **37**, 109928,  
292 doi:10.1016/j.celrep.2021.109928 (2021).
- 293 24 Liu, L. *et al.* Isolation and comparative analysis of antibodies that broadly neutralize  
294 sarbecoviruses. *bioRxiv*, doi:<https://doi.org/10.1101/2021.12.11.472236> (2021).
- 295 25 Barnes, C. O. *et al.* SARS-CoV-2 neutralizing antibody structures inform therapeutic  
296 strategies. *Nature* **588**, 682-687, doi:10.1038/s41586-020-2852-1 (2020).

- 297 26 Cerutti, G. *et al.* Potent SARS-CoV-2 neutralizing antibodies directed against spike N-  
298 terminal domain target a single supersite. *Cell Host Microbe* **29**, 819-833 e817,  
299 doi:10.1016/j.chom.2021.03.005 (2021).
- 300 27 Uriu, K. *et al.* Neutralization of the SARS-CoV-2 Mu Variant by Convalescent and  
301 Vaccine Serum. *N Engl J Med*, doi:10.1056/NEJMc2114706 (2021).
- 302 28 Annavajhala, M. K. *et al.* Emergence and expansion of SARS-CoV-2 B.1.526 after  
303 identification in New York. *Nature* **597**, 703-708, doi:10.1038/s41586-021-03908-2  
304 (2021).
- 305 29 Zhang, W. *et al.* Emergence of a Novel SARS-CoV-2 Variant in Southern California.  
306 *JAMA* **325**, 1324-1326, doi:10.1001/jama.2021.1612 (2021).
- 307 30 Faria, N. R. *et al.* Genomics and epidemiology of the P.1 SARS-CoV-2 lineage in  
308 Manaus, Brazil. *Science* **372**, 815-821, doi:10.1126/science.abh2644 (2021).
- 309 31 Tegally, H. *et al.* Detection of a SARS-CoV-2 variant of concern in South Africa. *Nature*  
310 **592**, 438-443, doi:10.1038/s41586-021-03402-9 (2021).
- 311 32 Andrews, N. *et al.* Effectiveness of COVID-19 vaccines against the Omicron (B.1.1.529)  
312 variant of concern. *medRxiv*, doi:<https://doi.org/10.1101/2021.12.14.21267615> (2021).
- 313 33 Wroughton, L. in *The Washington Post* (2021).
- 314 34 Kuhlmann, C. *et al.* Breakthrough Infections with SARS-CoV-2 Omicron Variant  
315 Despite Booster Dose of mRNA Vaccine. *SSRN*,  
316 doi:<https://dx.doi.org/10.2139/ssrn.3981711> (2021).
- 317 35 Garcia-Beltran, W. F. *et al.* mRNA-based COVID-19 vaccine boosters induce  
318 neutralizing immunity against SARS-CoV-2 Omicron variant. *medRxiv*,  
319 doi:<https://doi.org/10.1101/2021.12.14.21267755> (2021).
- 320 36 Cromer, D. *et al.* Neutralising antibody titres as predictors of protection against SARS-  
321 CoV-2 variants and the impact of boosting: a meta-analysis. *Lancet Microbe*,  
322 doi:10.1016/S2666-5247(21)00267-6 (2021).
- 323 37 Baym, M. *et al.* Inexpensive multiplexed library preparation for megabase-sized genomes.  
324 *PLoS One* **10**, e0128036, doi:10.1371/journal.pone.0128036 (2015).
- 325 38 Martin, M. Cutadapt Removes Adapter Sequences From High-Throughput Sequencing  
326 Reads. *EMBnet.journal* **17**, 10, doi:10.14806/ej.17.1.200 (2011).



327 39 Langmead, B. & Salzberg, S. L. Fast gapped-read alignment with Bowtie 2. *Nat Methods*  
328 **9**, 357-359, doi:10.1038/nmeth.1923 (2012).

329 40 Robinson, J. T. *et al.* Integrative genomics viewer. *Nat Biotechnol* **29**, 24-26,  
330 doi:10.1038/nbt.1754 (2011).

331 41 Chu, H. *et al.* Comparative tropism, replication kinetics, and cell damage profiling of  
332 SARS-CoV-2 and SARS-CoV with implications for clinical manifestations,  
333 transmissibility, and laboratory studies of COVID-19: an observational study. *Lancet*  
334 *Microbe* **1**, e14-e23, doi:10.1016/S2666-5247(20)30004-5 (2020).

335 42 Krissinel, E. & Henrick, K. Inference of macromolecular assemblies from crystalline  
336 state. *J Mol Biol* **372**, 774-797, doi:10.1016/j.jmb.2007.05.022 (2007).

337

338 **Methods**

339

340 **Serum samples**

341 Convalescent plasma samples were obtained from patients with documented SARS-CoV-2  
342 infection approximately one month after recovery or later. These samples were collected at the  
343 beginning of the pandemic in early 2020 at Columbia University Irving Medical Center, and  
344 therefore are assumed to be infection by the wild-type strain of SARS-CoV-2<sup>4</sup>. Sera from  
345 individuals who received two or three doses of mRNA-1273 or BNT162b2 vaccine were  
346 collected at Columbia University Irving Medical Center at least two weeks after the final dose.  
347 Sera from individuals who received one dose of Ad26.COV2.S or two doses of ChAdOx1 nCov-  
348 19 were obtained from BEI Resources. Some individuals were also infected by SARS-CoV-2 in  
349 addition to the vaccinations they received. Note that, whenever possible, we specifically chose  
350 samples with high titers against the wild-type strain of SARS-CoV-2 such that the loss in activity  
351 against B.1.1.529 could be better quantified, and therefore the titers observed here should be  
352 considered in that context. All collections were conducted under protocols reviewed and  
353 approved by the Institutional Review Board of Columbia University. Additional information for  
354 the vaccinee samples can be found in **Extended Data Table 1**.

355

356 **Monoclonal antibodies**

357 Antibodies were expressed as previously described<sup>22</sup>, by synthesis of VH and VL genes  
358 (GenScript), transfection of Expi293 cells (Thermo Fisher), and affinity purification from the  
359 supernatant by rProtein A Sepharose (GE). REGN10987, REGN10933, COV2-2196, and COV2-  
360 2130 were provided by Regeneron Pharmaceuticals, Brie-196 and Brie-198 were provided by Brie  
361 Biosciences, CB6 was provided by Baoshan Zhang and Peter Kwong (NIH), and 910-30 was  
362 provided by Brandon DeKosky (MIT).

363

364 **Variant SARS-CoV-2 spike plasmid construction**

365 An in-house high-throughput template-guide gene synthesis approach was used to generate spike  
366 genes with single or full mutations of B.1.1.529. Briefly, 5'-phosphorylated oligos with designed  
367 mutations were annealed to the reverse strand of the wild-type spike gene construct and extended  
368 by DNA polymerase. Extension products (forward-stranded fragments) were then ligated

369 together by Taq DNA ligase and subsequently amplified by PCR to generate variants of interest.  
370 To verify the sequences of variants, NGS libraries were prepared following a low-volume  
371 Nextera sequencing protocol<sup>37</sup> and sequenced on the Illumina Miseq platform (single-end mode  
372 with 50 bp R1). Raw reads were processed by Cutadapt v2.1<sup>38</sup> with default setting to remove  
373 adapters and then aligned to reference variants sequences using Bowtie2 v2.3.4<sup>39</sup> with default  
374 setting. Resulting reads alignments were then visualized in Integrative Genomics Viewer<sup>40</sup> and  
375 subjected to manual inspection to verify the fidelity of variants. Sequences of the oligos used in  
376 variants generation are provided in **Extended Data Table 2**.

377

### 378 **Pseudovirus production**

379 Pseudoviruses were produced in the vesicular stomatitis virus (VSV) background, in which the  
380 native glycoprotein was replaced by that of SARS-CoV-2 and its variants, as previously  
381 described<sup>24</sup>. Briefly, HEK293T cells were transfected with a spike expression construct with PEI  
382 (1 mg/mL) and cultured overnight at 37 °C under 5% CO<sub>2</sub>, and then infected with VSV-G  
383 pseudotyped ΔG-luciferase (G\*ΔG-luciferase, Kerafast) one day post-transfection. Following 2 h  
384 of infection, cells were washed three times, changed to fresh medium, and then cultured for  
385 approximately another 24 h before supernatants were collected, centrifuged, and aliquoted to use  
386 in assays.

387

### 388 **Pseudovirus neutralization assay**

389 All viruses were first titrated to normalize the viral input between assays. Heat-inactivated sera  
390 or antibodies were first serially diluted in 96 well-plates in triplicate. Viruses were then added  
391 and the virus-sample mixture was incubated at 37 °C for 1 h. Vero-E6 cells (ATCC) were then  
392 added at a density of  $3 \times 10^4$  cells per well and plates were incubated at 37 °C for approximately  
393 10 h. Luciferase activity was quantified by using the Luciferase Assay System (Promega)  
394 according to the manufacturer's instructions. Neutralization curves and IC<sub>50</sub> values were derived  
395 by fitting a non-linear five-parameter dose-response curve to the data in GraphPad Prism version  
396 9.2.

397

### 398 **Authentic virus isolation and propagation**

399 Authentic B.1.1.529 was isolated from a specimen from the respiratory tract of a COVID-19  
400 patient in Hong Kong by Kwok-Yung Yuen and colleagues at the Department of Microbiology,  
401 The University of Hong Kong. Isolation of wild-type SARS-CoV-2 was previously described<sup>41</sup>.  
402 Viruses were propagated in Vero-E6-TMPRSS2 cells and sequence confirmed by next-  
403 generation sequencing prior to use.

404

#### 405 **Authentic virus neutralization assay**

406 To measure neutralization of authentic SARS-CoV-2 viruses, Vero-E6-TMPRSS2 cells were  
407 first seeded in 96 well-plates in cell culture media (DMEM + 10% FBS + 1%  
408 penicillin/streptomycin) overnight at 37 °C under 5% CO<sub>2</sub> to establish a monolayer. The  
409 following day, sera or antibodies were serially diluted in 96 well-plates in triplicate in DMEM +  
410 2% FBS and then incubated with 0.01 MOI of wild-type SARS-CoV-2 or B.1.1.529 at 37 °C for  
411 1 h. Afterwards, the mixture was overlaid onto cells and further incubated at 37 °C under 5%  
412 CO<sub>2</sub> for approximately 72 h. Cytopathic effects were then visually assessed in all wells and  
413 scored as either negative or positive for infection by comparison to control uninfected or infected  
414 wells in a blinded manner. Neutralization curves and IC<sub>50</sub> values were derived by fitting a non-  
415 linear five-parameter dose-response curve to the data in GraphPad Prism version 9.2.

416

#### 417 **Antibody footprint analysis and RBD mutagenesis analysis**

418 The SARS-CoV-2 spike structure used for displaying epitope footprints and mutations within  
419 emerging strains was downloaded from PDB (PDBID: 6ZGE). The structures of antibody-spike  
420 complexes were also obtained from PDB (7L5B for 2-15, 6XDG for REGN10933 and  
421 REGN10987, 7L2E for 4-18, 7RW2 for 5-7, 7C01 for CB6, 7KMG for LY-COV555, 7CDI for  
422 Brij-196, 7KS9 for 910-30, 7LD1 for DH1047, 7RAL for S2X259, 7LSS for 2-7, and 6WPT for  
423 S309). Interface residues were identified using PISA<sup>42</sup> using default parameters. The footprint  
424 for each antibody was defined by the boundaries of all epitope residues. The border for each  
425 footprint was then optimized by ImageMagick 7.0.10-31 (<https://imagemagick.org>). PyMOL  
426 2.3.2 was used to perform mutagenesis and to make structural plots (Schrödinger).

427

428 **Acknowledgements**

429 We are grateful Regeneron Pharmaceuticals, B. Zhang and P. Kwong (NIAID), and B. Dekosky  
430 (MIT) for antibodies. This study was supported by funding from the Gates Foundation, JPB  
431 Foundation, Andrew and Peggy Cherng, Samuel Yin, Carol Ludwig, David and Roger Wu,  
432 Health@InnoHK, and the National Science Foundation (MCB-2032259).

433

434 **Author contributions**

435 D.D.H. conceived this project. L.H.L., S.I., and M.W. conducted pseudovirus neutralization  
436 experiments. J.F-W.C., H.C., K.K-H.C., T.T-T.Y., C.Y., K.K-W.T., and H.C. conducted  
437 authentic virus neutralization experiments. Y.G. and Z.Z. conducted bioinformatic analyses.  
438 L.Y.L. and Y.M.H. constructed the spike expression plasmids. Y.L. managed the project. J.Y.  
439 expressed and purified antibodies. M.T.Y. and M.E.S. provided clinical samples. M.S.N. and  
440 Y.X.H. contributed to discussions. H.H.W., K-Y.Y., and D.D.H. directed and supervised the  
441 project. L.H.L., S.I., and D.D.H. analyzed the results and wrote the manuscript.

442

443 **Competing interests**

444 L.L., S.I., M.S.N., J.Y., Y.H., and D.D.H. are inventors on patent applications on some of the  
445 antibodies described in this manuscript.

446

447 **Data and materials availability**

448 All data are provided in the paper or the Supplementary Information.

449